

# Geophysical Research Letters<sup>®</sup>

## RESEARCH LETTER

10.1029/2023GL105475

## How Does the Southern Annular Mode Control Surface Melt in East Antarctica?



### Key Points:

- Modeled surface meltwater fluxes on East Antarctic ice shelves are negatively correlated with the Southern Annular Mode (SAM) index
- Melt fluxes increase for a decreasing SAM index owing to reduced precipitation in Dronning Maud Land, and a warmer atmosphere in Wilkes Land
- The SAM-melt relationship is stronger in December than January, highlighting the importance of the snowmelt-albedo feedback

### Supporting Information:

Supporting Information may be found in the online version of this article.

### Correspondence to:

D. Saunderson,  
[dominic.saunderson@monash.edu](mailto:dominic.saunderson@monash.edu)

### Citation:

Saunderson, D., Mackintosh, A. N., McCormack, F. S., Jones, R. S., & van Dalum, C. T. (2024). How does the Southern Annular Mode control surface melt in East Antarctica? *Geophysical Research Letters*, *51*, e2023GL105475. <https://doi.org/10.1029/2023GL105475>

Received 20 OCT 2023

Accepted 20 FEB 2024

### Author Contributions:

**Conceptualization:** Dominic Saunderson

**Data curation:** Christiaan T. van Dalum

**Formal analysis:** Dominic Saunderson

**Funding acquisition:** Andrew N. Mackintosh, Felicity S. McCormack, Richard S. Jones



**Methodology:** Dominic Saunderson, Andrew N. Mackintosh, Felicity S. McCormack, Richard S. Jones

**Software:** Dominic Saunderson  
**Supervision:** Andrew N. Mackintosh, Felicity S. McCormack, Richard S. Jones

**Visualization:** Dominic Saunderson

**Writing – original draft:**

Dominic Saunderson

**Dominic Saunderson**<sup>1</sup> , **Andrew N. Mackintosh**<sup>1</sup>, **Felicity S. McCormack**<sup>1</sup>, **Richard S. Jones**<sup>1</sup> , and **Christiaan T. van Dalum**<sup>2</sup>

<sup>1</sup>Securing Antarctica's Environmental Future, School of Earth, Atmosphere and Environment, Monash University, Clayton, VIC, Australia, <sup>2</sup>Institute for Marine and Atmospheric Research, Utrecht University, Utrecht, The Netherlands

**Abstract** Surface melt in East Antarctica is strongly correlated with the Southern Annular Mode (SAM) index, but the spatiotemporal variability of the relationship, and the physical processes responsible for it, have not been examined. Here, using melt flux estimates and climate variables from the RACMO2.3p3 regional climate model, we show that a decreasing SAM index is associated with increased melt in Dronning Maud Land primarily owing to reduced precipitation and greater absorption of solar radiation. Conversely, in Wilkes Land, a decreasing SAM index corresponds to increased melt because of greater incoming longwave radiation from a warmer atmosphere. We also demonstrate that SAM-melt correlations are strongest in December as the melt season develops, and that the SAM's influence on peak melt intensities in January occurs indirectly through the snowmelt-albedo feedback. Future work must account for such variability in the physical processes underlying the SAM-melt relationship to reduce uncertainty in surface melt projections.

**Plain Language Summary** The Southern Annular Mode (SAM) index describes the strength and location of the westerly winds in the Southern Hemisphere. It has previously been linked to interannual variability in the number of satellite-observed melt days on the surface of East Antarctica's floating ice shelves. Here, we use melt estimates from a regional climate model adapted for the polar regions to show that the SAM-melt relationship is also observed for meltwater fluxes, and to identify the influence of the SAM on the different energy sources driving surface melt. We find that a more negative SAM index (weaker westerlies) is associated with higher air temperatures across most of East Antarctica, and leads to increased incoming longwave radiation and sensible heat fluxes in Wilkes Land. In contrast, in Dronning Maud Land (DML), incoming longwave radiation is unaffected by the SAM, leading to net longwave energy losses, and sensible heat fluxes are reduced because of weaker surface winds. Instead, greater melt in DML is driven through increased absorption of solar radiation, owing to reduced precipitation and a darker surface. We also find differences in the strength of the SAM-melt relationship on both sub-seasonal and decadal timescales.

## 1. Introduction

Antarctic ice shelves are floating extensions of the ice sheet, surrounding ~75% of the continent (Bindschadler et al., 2011) and providing a buttressing force that slows the flow of grounded ice to the ocean (Fürst et al., 2016; Reese et al., 2018). If the buttressing force is reduced, Antarctica's contribution to global sea level rise could increase dramatically (Oppenheimer et al., 2019; Sun et al., 2020), making it critical to understand the processes, such as surface melt, that can cause an ice shelf to weaken and disintegrate.

Surface melt can instigate the loss of ice shelves because it reduces pore space in the overlying firn layer (Ligtenberg et al., 2014; Munneke et al., 2014), potentially leading to meltwater ponds (Arthur et al., 2020; Leeson et al., 2020; van Wessem et al., 2023), hydrofracture (van der Veen, 1998; Weertman, 1973), and, in extreme cases, ice shelf collapse (Banwell et al., 2013; MacAyeal et al., 2003; Robel & Banwell, 2019). Meltwater-driven disintegration is particularly associated with the unique melt environment of the Antarctic Peninsula (Laffin et al., 2022; Morris & Vaughan, 2003; Scambos et al., 2000, 2009), but the loss of the Voyeykov (Arthur et al., 2021) and Conger (Lhermitte et al., 2023; Wille et al., 2024) Ice Shelves shows that East Antarctic ice shelves are also vulnerable to collapse. Although the latter two collapses were not directly driven by surface meltwater, the projected increase in surface melt rates under a warmer climate (Gilbert & Kittel, 2021; Trusel et al., 2015) suggests that the risk of meltwater-driven collapse will increase, necessitating further research into the processes controlling surface melt, and especially in East Antarctica, which holds approximately 90% of Antarctica's sea level rise equivalent (Morlighem et al., 2020).

© 2024. The Authors.

This is an open access article under the terms of the [Creative Commons Attribution License](https://creativecommons.org/licenses/by/4.0/), which permits use, distribution and reproduction in any medium, provided the original work is properly cited.

**Writing – review & editing:**

Dominic Saunderson, Andrew  
N. Mackintosh, Felicity S. McCormack,  
Richard S. Jones, Christiaan T. van Dalum

Variability in the occurrence, extent, and intensity of surface melt arises from controls across multiple spatio-temporal scales. Spatially, Antarctica's geography (e.g., latitude and topography) and localized melt processes (e.g., surface winds and albedo) are important controls on surface melt (Jakobs et al., 2021; Lenaerts et al., 2017; Saunderson et al., 2022; Tedesco et al., 2007), whilst the temporal variability is strongly influenced by large-scale modes of atmospheric variability, particularly including the Southern Annular Mode (SAM) (Johnson et al., 2022; Tedesco & Monaghan, 2009; Torinesi et al., 2003).

The SAM is the leading mode of extratropical climate variability in the Southern Hemisphere on daily-to-decadal timescales, and is observed as a near-zonally symmetric, ring-like pattern in atmospheric pressure levels (Fogt & Marshall, 2020). Positive SAM indices represent an increased pressure gradient between the mid (~40°S) and high (~65°S) latitudes, producing stronger westerly winds that are closer to Antarctica. For negative SAM indices, the westerlies weaken and relax equatorward.

In East Antarctica, strong negative correlations exist between the SAM index and melt metrics such as the melt extent (Tedesco & Monaghan, 2009) and duration (Johnson et al., 2022). However, such studies rely on satellite observations to define melt and thus focus on the extent and occurrence of melt rather than its intensity (i.e., meltwater production). This distinction is important because strongly non-linear relationships can exist between the number of melt days and total meltwater fluxes (Banwell et al., 2023), and it is the latter which is critical when considering the firn air content of an ice shelf and the likelihood of meltwater ponding and hydrofracture (Alley et al., 2018; Lai et al., 2020; van Wessem et al., 2023). Furthermore, the mechanisms through which the SAM influences the surface melt conditions, and the spatiotemporal variability of the SAM-melt relationship, have not previously been considered in detail. To address these gaps, we use modeled surface meltwater fluxes and climate variables from the RACMO2.3p3 regional climate model (van Dalum et al., 2022), and investigate the influence of the SAM on surface melt for 27 East Antarctic ice shelves over the last four decades (1980–2018).

## 2. Datasets and Models

### 2.1. RACMO2.3p3

We examine monthly and daily variables from the polar version of the RACMO2 regional climate model, including surface melt; turbulent, radiative, and conductive heat fluxes; surface (10m) winds; and surface (2m) air temperatures ( $T_{2m}$ ) (van Dalum et al., 2021). RACMO2 has been used extensively in studies of Antarctica's surface climate (e.g., Jakobs et al., 2021; Lenaerts et al., 2012, 2018; van Wessem et al., 2014, 2018), and the latest version (RACMO2.3p3) contains two key improvements for modeling surface melt: 1) an updated spectral snow and ice albedo scheme, which permits subsurface penetration of shortwave radiation; and 2) an updated multi-layer firn module that includes a finer vertical resolution near the surface where melt occurs (van Dalum et al., 2019, 2020, 2022). The model is initialized using a snowpack from a previous model run, and run over the period 1979–2018; data until 1984 are considered model spin-up, but results are consistent between the two periods, and thus we report values for the full dataset (i.e., summers 1979/1980–2017/2018). The model is run on a 27 km grid across Antarctica, and forced at the boundaries by 3-hourly ERA5 reanalysis data (Hersbach et al., 2020).

### 2.2. Ice Shelves

For individual ice shelf-based calculations, we include only RACMO pixels that are at least 50% ice shelf according to the MEaSUREs Antarctic Boundaries dataset (Version 2) (Mouginot et al., 2017; Rignot et al., 2013). Only East Antarctic ice shelves containing at least two pixels meeting this criteria are included, resulting in 27 ice shelves suitable for analysis (Figure 1; Table S1 in Supporting Information S1). We group these ice shelves into six regions based on their proximity and the similarity of their response to the SAM (e.g., Figures 2 and 3); west-to-east, these regions are: Weddell; Dronning Maud Land; Amery; Wilkes Land; Oates-George V; and Ross.

### 2.3. SAM Indices

We use the monthly and daily SAM index provided by the NOAA Climate Prediction Center (hereafter the NOAA SAM index). This index is derived from an EOF analysis of 700 hPa geopotential height anomalies in NCEP/NCAR reanalysis data (Mo, 2000). Daily values are averaged using a 9-day running mean, because the SAM has an approximate 10-day decorrelation period (Robinson, 2000), and plotted against the window

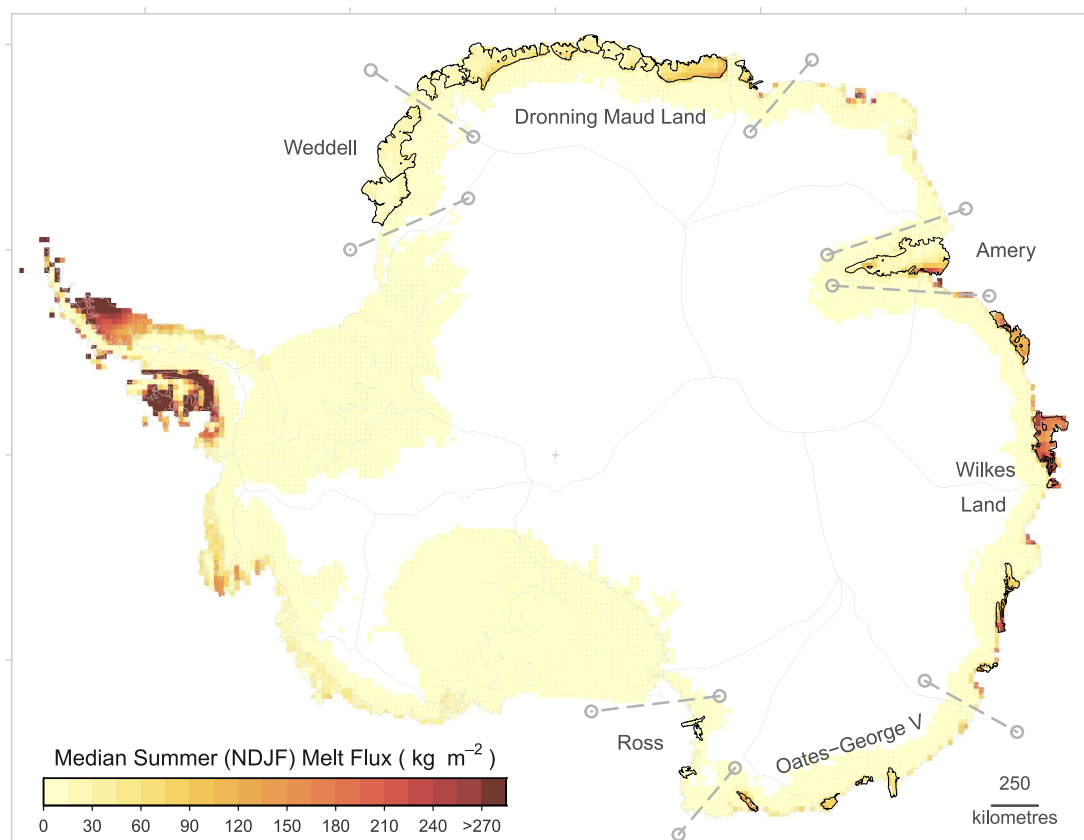


**Figure 1.** Median summer (NDJF) RACMO melt fluxes ( $\text{kg m}^{-2} \text{ summer}^{-1}$ ) (1980–2018). Dashed lines separate the 27 ice shelves (outlined in black; Table S1 in Supporting Information S1) into six regions; gray lines delineate IMBIE drainage basins (Mouginot et al., 2017). Stippling indicates statistically insignificant ( $p > 0.05$ ) correlations between melt fluxes and satellite-observed melt days (Picard, 2022); the absence of stippling over East Antarctic ice shelves demonstrates good interannual agreement between satellite observations and modeled melt fluxes.

midpoint. We also use the monthly station-based SAM index of Marshall (2003) in a sensitivity analysis. All time-series are linearly detrended before correlation and regression analysis; statistical significance is tested using a two-tailed Pearson’s Product-Moment Correlation test against a null hypothesis of zero correlation.

### 3. Spatial and Interannual Variability in Surface Melt Fluxes

Surface melt fluxes vary greatly in both time and space for East Antarctic ice shelves (Figures 1 and 2c). The highest median melt fluxes (November–February) occur in Wilkes Land ( $\sim 70\text{--}245 \text{ kg m}^{-2} \text{ summer}^{-1}$ ), whereas the lowest occur on the ice shelves closest to West Antarctica, in the Ross and Weddell regions ( $\sim 5\text{--}20 \text{ kg m}^{-2} \text{ summer}^{-1}$ ). The modeled melt fluxes compare well with satellite-derived estimates (1999–2009) (Trusel et al., 2013), and correlate strongly ( $r = 0.4\text{--}0.8$ ;  $p < 0.05$ ) with the number of satellite-observed melt days each summer for nearly all ice shelf pixels (Figure 1). We also find that, on average, more than 95% of an ice shelf’s total melt each summer occurs in December and January (DJ) (Table S1 in Supporting Information S1; Figure 2c), and thus we focus on these two months from hereon in unless explicitly stated.

Plotting the DJ total melt fluxes as percentiles for each ice shelf (Figure 2c) shows a general agreement across all East Antarctic ice shelves over whether melt fluxes are above or below average in any given summer. The East Antarctic-wide similarity is particularly evident in the below-average melt through the 1990s, culminating in 1999/2000 when nearly all ice shelves experienced their lowest melt flux over the study period. Greater regional variability exists when considering the highest melt fluxes. For example, the highest melt fluxes in Dronning Maud Land occur in 1984/1985, but in 2013/2014 in the Ross region. Nevertheless, across the majority of the 27 ice shelves, there is a general agreement in the percentiles each summer, suggesting that the interannual variability

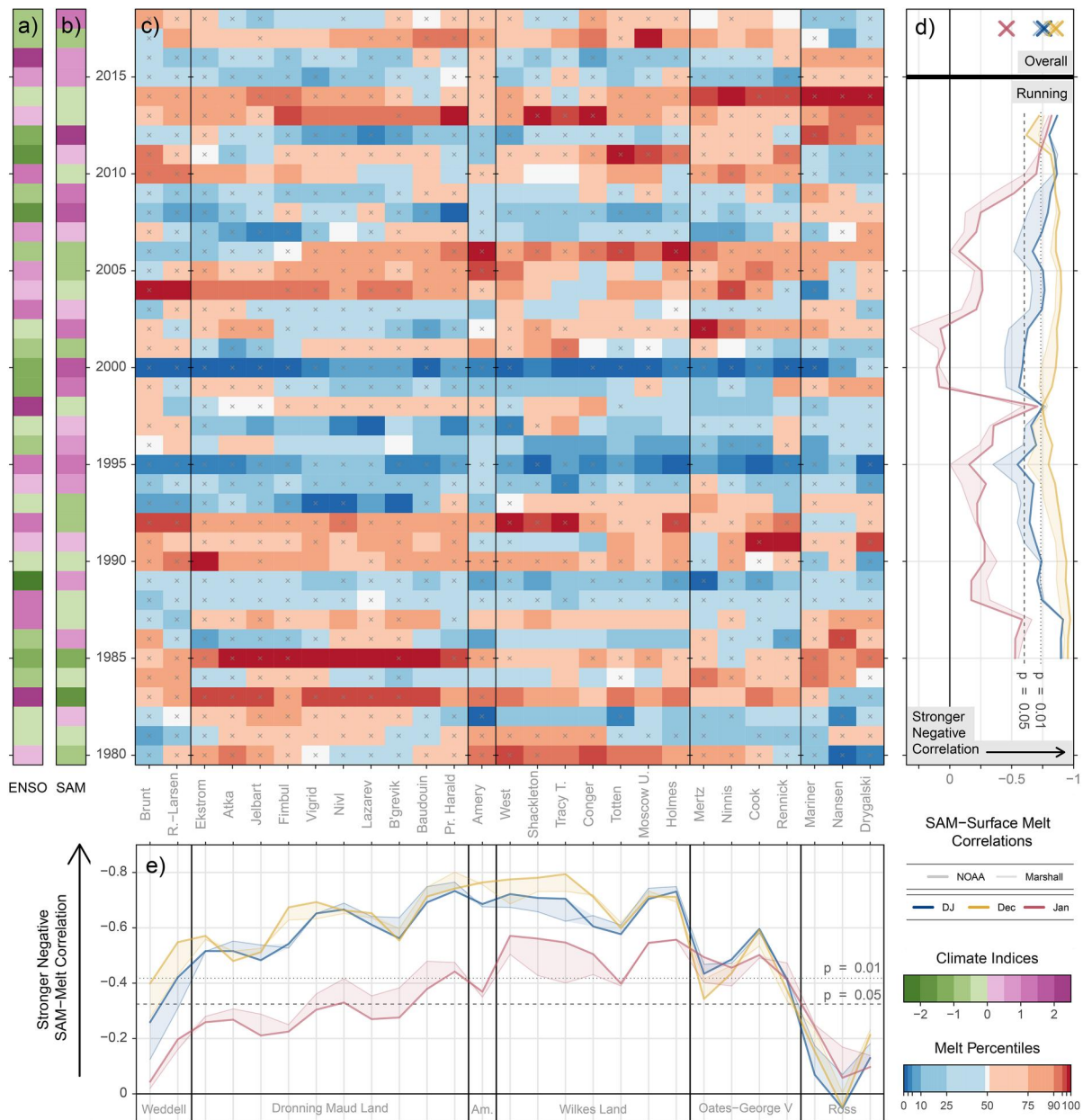


**Figure 2.** Interannual variability in the NOAA (a) ENSO3.4 (Oct–Jan) and (b) SAM (Dec–Jan) indices. (c) RACMO-modeled melt fluxes (Dec–Jan) for 27 East Antarctic ice shelves, plotted as percentiles; red values are above the median for each ice shelf, and blue below. Crosses indicate >95% of a summer’s melt occurred in December and January. (d) East Antarctic-averaged melt fluxes correlated with the SAM indices, across the full period (1980–2018; crosses) and using an 11-year running correlation (lines). (e) SAM–melt correlations for the 27 ice shelves, ordered (left-to-right) west-to-east.

in East Antarctic surface melt is driven by large-scale atmospheric controls, such as the SAM and/or the El Niño–Southern Oscillation (ENSO).

Comparing Figures 2a and 2c shows that the ENSO–melt relationship is not straightforward, with different melt responses evident in the three strongest El Niño events during the study period. For example, in 1982/1983, melt fluxes are above-average for nearly all ice shelves in East Antarctica, often reaching the 90th or 95th percentiles, particularly in Dronning Maud Land. In contrast, in 2015/2016, below-average melt fluxes occur on nearly all ice shelves outside the Ross region, whilst in 1997/1998, melt fluxes are close to their median values but vary regionally as to whether they are above or below average. These three summers all have different SAM conditions (DJ-averaged NOAA SAM index =  $-1.64$ ,  $1.00$ ,  $-0.21$ ), showing that the SAM index is a better predictor of

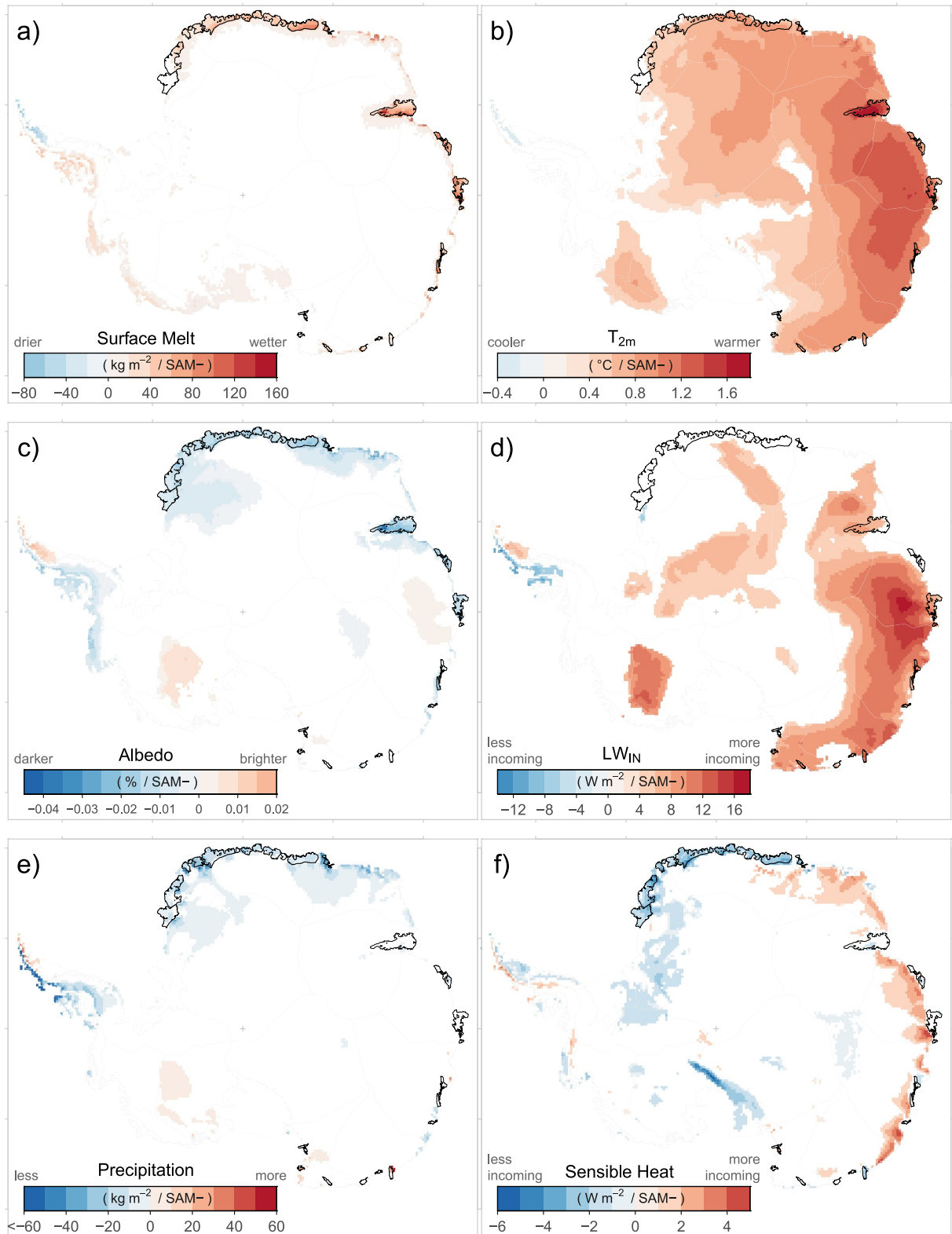


**Figure 3.** Regressions against the NOAA SAM index for RACMO-modeled variables, based on December–January values (1980–2018); only statistically significant regressions ( $p < 0.05$ ) over the ice sheet are shown. See Figures S2–S4 in Supporting Information S1 for additional variables.

surface melt than ENSO, and a general negative relationship between surface melt and the SAM index is evident when comparing Figures 2b and 2c. We now investigate this relationship in detail.

## 4. Influence of the Southern Annular Mode

### 4.1. SAM-Melt Correlations

Strong, statistically significant negative correlations ( $-0.8 < r < -0.4$ ;  $p < 0.01$ ) exist between DJ melt fluxes and both SAM indices for all ice shelves from Dronning Maud Land to the Oates-George V region (Figure 2e), and also for an East Antarctic-wide average (Figure 2d), but not in the Ross region. SAM-melt correlations also vary over time (Figure 2d), with very high correlations for both indices in the 1980s and 2010s ( $r < -0.75$ ) occurring either side of weaker, sometimes statistically insignificant correlations in the late 1990s and early 2000s, when melt rates were low. Overall, both SAM indices produce similar correlation values, with the stronger correlation differing between ice shelves, but the reanalysis (i.e., NOAA) index is higher when considering the East Antarctic-wide average.

We find that correlations using the DJ-averaged SAM are greater than those of the October–January period previously used in the literature (Johnson et al., 2022; Tedesco & Monaghan, 2009; Torinesi et al., 2003). Stronger DJ correlations in our analysis (Figure S1a in Supporting Information S1) are likely because previous work has examined the SAM-melt relationship at a continental scale, and thus included the Antarctica Peninsula, where the melt season begins earlier and the SAM has a strong impact on foehn winds (Cape et al., 2015; Marshall et al., 2006). The lack of statistically significant correlations between the October or November SAM and summer melt (Figure S1b in Supporting Information S1), plus the stronger DJ correlations, indicates that surface melt in East Antarctica is influenced by the summer (DJ) SAM rather than being a lagged response to the late spring (October–November) SAM.

### 4.2. Physical Mechanisms Connecting SAM and Surface Melt

To investigate the physical mechanisms driving the SAM-melt relationship, we linearly regress RACMO climate variables against the NOAA SAM index each summer (DJ) (Figure 3 and Figure S2–S4 in Supporting Information S1). Statistically significant ( $p < 0.05$ ) SAM-melt regressions occur for nearly all pixels on East Antarctic ice shelves, except those closest to West Antarctica, and are also present (albeit much weaker) beyond the ice shelves for much of the coastline west of the Shackleton Ice Shelf (Figure 3a). We therefore perform the regression analysis across all of Antarctica, and not just on the 27 selected ice shelves. Because the SAM-melt correlations are negative (Figures 2d and 2e), we report the changes in each variable associated with a unit decrease in the SAM index (SAM-) (e.g., from a SAM index of 0 to  $-1$ ).

A negative SAM- $T_{2m}$  relationship is widespread across all of East Antarctica (Figure 3b). The strongest temperature responses to a decreasing SAM index occur in the Wilkes Land and Amery regions ( $1$ – $1.75^{\circ}\text{C}/\text{SAM-}$ ), where SAM variability explains 40%–70% of the  $T_{2m}$  variability (Figure S3b in Supporting Information S1). Weaker SAM- $T_{2m}$  regressions ( $0.25$ – $1^{\circ}\text{C}/\text{SAM-}$ ) occur outside these two regions, but remain statistically significant except on the two ice shelves closest to West Antarctica. A warmer atmosphere can contribute to an increase in surface melt through greater incoming longwave radiation and sensible heat fluxes (Braithwaite & Olesen, 1990; Hock, 2005; Ohmura, 2001), and the negative SAM- $T_{2m}$  relationship in Antarctica has previously been attributed to two factors.

First, the weakened westerlies during a negative SAM phase allow increased meridional flow of heat to Antarctica from the mid-latitudes (Marshall & Thompson, 2016; Previdi et al., 2013). In our analysis, widespread increases in the incoming longwave radiation, consistent with a warmer atmosphere, occur across the Amery, Wilkes Land and Oates-George V regions as the SAM index decreases (Figure 3d). In the latter two regions, the longwave gains offset greater outgoing longwave radiation (from a warmer surface), meaning the net longwave budget is approximately balanced and varies insignificantly with the SAM index (Figure S2d in Supporting Information S1). In contrast, on the Amery Ice Shelf, the increased longwave gains are insufficient to offset the greater losses, and the net longwave budget is thus a greater heat sink as the SAM index decreases. Greater net longwave losses also occur in the Dronning Maud Land and Weddell regions, where there is no significant change in incoming longwave radiation associated with a decreasing SAM index, but there are greater losses (Figure S2c in Supporting Information S1).

Second, the magnitude of atmospheric pressure increases associated with a decreasing SAM index differs across Antarctica (Figure S2f in Supporting Information S1). Greater pressure increases occur over the Antarctic interior than at the coastline, enhancing the pole-to-coast pressure gradient and leading to stronger surface winds in the regions where this gradient aligns with the prevailing easterly winds (Figure S4c in Supporting Information S1) (van den Broeke & van Lipzig, 2004; Neme et al., 2022). Stronger winds disrupt the near-surface temperature inversion, and increase turbulent heat fluxes. Consistent with this hypothesis, our analysis shows greater wind speeds, latent heat losses, and sensible heat gains in Wilkes Land, where the greatest  $T_{2m}$  changes occur, although changes in sensible heat are statistically insignificant over the ice shelves themselves (Figure 3f). Conversely, in the Weddell and Dronning Maud Land regions, the prevailing easterly winds are opposed by a westerly pressure gradient from the high pressure anomaly in the Weddell Sea (Figure S2f in Supporting Information S1), leading to weaker surface winds (Figure S4b in Supporting Information S1) and subsequently reduced sensible heat gains in these regions (Figure 3f).

Despite greater longwave and turbulent heat losses in the Weddell and Dronning Maud Land regions, a decreasing SAM index corresponds to greater surface melt in these regions (Figure 3a). The increases are driven by greater net shortwave radiation (Figure S2b in Supporting Information S1), owing to reduced precipitation (Figure 3e) and a lower surface albedo (Figure 3c). Precipitation acts to raise the albedo and cool the surface (Picard et al., 2012), inhibiting melt. Reduced snowfall therefore allows the surface albedo to be progressively lowered via the positive snowmelt-albedo feedback: as the surface melts, liquid water reduces the surface albedo by enlarging the snow grains, causing increased absorption of shortwave radiation and driving further melt (Jakobs et al., 2021; Wiscombe & Warren, 1980). The lowered surface albedo (also observed in the Amery and Wilkes regions) is thus both a cause and effect of the enhanced melt associated with a decreasing SAM index. The potency of the feedback is particularly evident when noting that the greatest increases occur on the Amery, Baudouin and Shackleton Ice Shelves, where strong wind scour has exposed low albedo blue ice (Hui et al., 2014; Lenaerts et al., 2017).

### 4.3. Subseasonal Variability

On a monthly basis, the SAM-melt relationship is stronger in December than January for all ice shelves beyond the Ross or Oates-George V regions (Figure 2e). Daily datasets show that the strongest SAM-melt correlations occur around the summer solstice (Figure 4a), when incoming solar radiation is greatest (Figure S5c in Supporting Information S1) and when the SAM index also significantly correlates with  $T_{2m}$  and surface albedo (Figure S6 in Supporting Information S1). In contrast, surface melt,  $T_{2m}$ , and incoming longwave radiation are greatest, and albedo lowest, in early-mid January (Figures 4b and 4d & Figure S5 in Supporting Information S1), when the corresponding correlations with the SAM index are reduced (Figure S6 in Supporting Information S1). These results suggest that the conditions necessary for melt are usually already present in the January climatology, and are less dependent on the SAM, whereas changes in the SAM are an important control on when (or whether) the conditions for melt onset occur in December.

Furthermore, the similarity of the December and DJ SAM-melt correlations (Figures 2d and 2e) shows that the December SAM is important in determining the full summer's melt. This influence is explained by the snowmelt-albedo feedback, which results in January having lower average albedo values than December (Figure 4d) but greater interannual variability (Figure S7 in Supporting Information S1). Indeed, using the SAM index from a month prior to the peak of the melt season improves the SAM-melt correlation in the Weddell, Dronning Maud Land, and Amery regions (Figure 4c), showing the importance of this feedback in these regions, and providing an indirect link between the SAM and peak melt intensities.

## 5. Discussion

Our findings support recent work highlighting the influence of the SAM on surface melt in East Antarctica by showing that strong SAM-melt relationships exist for modeled meltwater fluxes as well as satellite-derived melt metrics (Johnson et al., 2022) and melt proxies from climate models (Orr et al., 2023). Establishing the relationship between the SAM and surface melt fluxes is important because accurate melt flux estimates, and their magnitude relative to precipitation, are key to determining whether melt ponds will form (Pfeffer et al., 1991; van Wessem et al., 2023). Under a warmer climate, both surface melt and precipitation are expected to increase in Antarctica (Gilbert & Kittel, 2021; Kittel et al., 2021; Nicola et al., 2023), although the relative magnitude, rates,

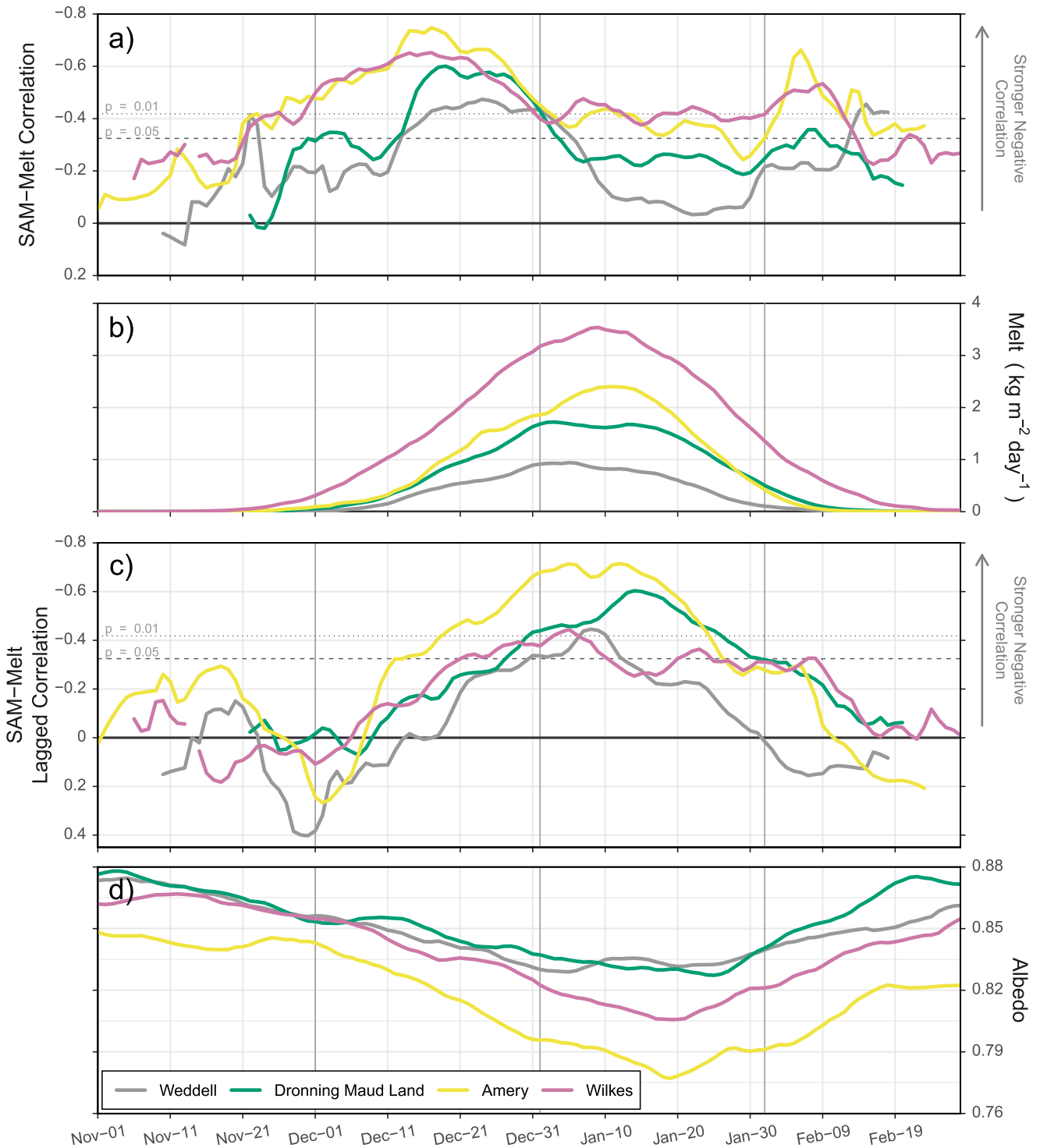


**Figure 4.** (a) SAM-melt correlations; (b) mean surface melt fluxes; (c) 28-day lagged SAM-melt correlations; and (d) mean surface albedo plotted through the melt season. Plots use 9-day running means of the NOAA SAM index and RACMO model output (1980–2018).

and spatial homogeneity of the changes remain uncertain. Future work investigating the processes controlling surface melt should therefore also consider the associated impacts on precipitation, and it is vital that in-situ observations are made in key melt locations to verify both modeled and satellite-derived estimates of melt and precipitation.



The majority of East Antarctica's surface melt occurs on ice shelves (Figure 1). However, some surface melt does occur on grounded ice, and the amount, whilst much less than on the ice shelves, is also often significantly correlated with the SAM index (Figure 3a). We further find that for a decreasing SAM index, the greatest increases in  $T_{2m}$ , sensible heat, and incoming longwave radiation do not occur over the ice shelves, but inland in Wilkes Land (Figure 3), which is currently melt-free year-round (Figure 1). In the future, it is possible that melt may become more widespread and reach such higher elevation areas away from the coast, as can already occur in Greenland (Box et al., 2022; Nghiem et al., 2012) and West Antarctica (Wille et al., 2019), and our findings suggest that the SAM would remain an important control on such melt.

Our analysis focuses on December and January, when the majority (>95%) of melt occurs (Table S1 in Supporting Information S1; Figure 2c). We find that the SAM-melt relationship is stronger in December than January (Figure 2e), and also slightly increases again in early February, particularly in the Amery and Wilkes Land regions (Figure 4a). The lower correlations in January are likely because the climatology is already more susceptible to melt (Figure 4 and Figure S5 in Supporting Information S1), and because of the non-linearity introduced by the snowmelt-albedo feedback (Jakobs et al., 2021). This finding suggests that the SAM could be more influential during the development, and possibly cessation, of the melt season than at its peak, and future work should investigate whether the SAM-melt relationship remains robust at the height of the melt season in a warmer climate.

Although we focus exclusively on the SAM-melt relationship in this work, other modes of atmospheric variability can be potentially important controls. For example, the influence of ENSO on surface melt has been identified, particularly in West Antarctica (Scott et al., 2019; Tedesco & Monaghan, 2009). However, the ENSO-melt relationship is complex (Section 3), and the melt response to ENSO can vary dramatically around Antarctica; for example, during the strong El Niño summer of 2015/2016, melt was unusually prolonged and extensive in West Antarctica (Nicolas et al., 2017; Zou et al., 2019) but melt fluxes were below-average in East Antarctica (Figure 2c). Previous work has also shown that the phase of the Zonal Wave 3 (ZW3) pattern can control spatial variability in meridional heat transport around Antarctica, as evidenced by sea ice anomalies (Goyal et al., 2022; Raphael, 2004), but it is unknown whether a similar influence also occurs for surface melt. Future work needs to account for such regional variability in the surface melt response, and to investigate how atmospheric circulation patterns such as ENSO and ZW3 influence the zonal asymmetry of the SAM (Campitelli et al., 2022; Fogt et al., 2012) and modulate the SAM-melt relationship. Similarly, a better understanding of events such as atmospheric rivers (Wille et al., 2019, 2022), and their relationship to modes of climate variability including the SAM, could be critical for predicting the likelihood and magnitude of extreme melt events, and should be the focus of future work.

Over recent decades, the summer SAM has trended positive because of ozone depletion and increased greenhouse gas emissions (Arblaster & Meehl, 2006; Fogt & Marshall, 2020; King et al., 2023; Polvani et al., 2011). The trend has slowed as the ozone hole recovers (Zheng, 2024) and would potentially reverse (Arblaster et al., 2011), but a positive-trending SAM is projected by the late 21st century under increased greenhouse gas emissions (Deng et al., 2022; Simpkins & Karpechko, 2012). Combined with our findings, these trends suggest that the SAM has likely suppressed surface melt in East Antarctica over the satellite era, and could continue to do so in the coming century. Nevertheless, our work has shown that the SAM-melt relationship in East Antarctica varies in time and space, and caution therefore needs to be taken when using the SAM index as a simple proxy for surface melt, particularly in a warming climate. By examining the underlying physical processes that drive the contemporary SAM-melt relationship, our work provides insights that allow a more robust consideration of future surface melt projections in East Antarctica. Future work also needs to account for the influence of other controls on surface melt, such as ENSO, ZW3, and atmospheric rivers, and their interactions with the SAM, as well as determining how the impact of a positive-trending (i.e., melt-suppressing) SAM balances against a warming (i.e., melt-enhancing) climate.

### Data Availability Statement

The RACMO2.3p3 datasets (van Dalum et al., 2021) are available online at: <https://doi.org/10.5281/zenodo.7639053>. Ice shelves are defined according to the MEaSURES Antarctic Boundaries dataset, Version 2 (Mouginot et al., 2017), which is available online at: <https://doi.org/10.5067/AXE4121732AD>. Two SAM indices are

used throughout this work. The Marshall (2003) SAM index is available online from the British Antarctic Survey (BAS) at: <http://www.nerc-bas.ac.uk/public/icd/gjma/newsam.1957.2007.txt>. The NOAA SAM index is available online from the NOAA Climate Prediction Centre (CPC) at: [https://www.cpc.ncep.noaa.gov/products/precip/CWlink/daily\\_ao\\_index/ao/ao.shtml](https://www.cpc.ncep.noaa.gov/products/precip/CWlink/daily_ao_index/ao/ao.shtml). The NOAA ENSO3.4 index used in Figure 2a is available online from the Physical Science Laboratory (PSL) at: [https://psl.noaa.gov/gcos\\_wgsp/Timeseries/Data/nino34.long.anom.data](https://psl.noaa.gov/gcos_wgsp/Timeseries/Data/nino34.long.anom.data). The ERA5 reanalysis data (Hersbach et al., 2020) used in Figure S2f in Supporting Information S1 is available online from the Copernicus Climate Change Service (C3S) Climate Data Store (CDS) at: <https://cds.climate.copernicus.eu/cdsapp#!/dataset/reanalysis-era5-single-levels-monthly-means>. The AMSR melt observations (Picard, 2022) used in Figure 1 are available online at: <https://doi.org/10.18709/PERSCIDO.2022.09.DS376>. All data analysis and figure preparation was performed using the R programming language (R Core Team, 2023), and relied heavily on the *terra* (Hijmans et al., 2023), *khroma* (Frerebeau et al., 2024), and *devtools* (Wickham et al., 2022) packages. The R code can be accessed online at: <https://doi.org/10.26180/24319153.v2>.

### Acknowledgments

DS, ANM, FSM and RSJ were supported under the Australian Research Council (ARC) Special Research Initiative (SRI) Securing Antarctica's Environmental Future (SR200100005). DS was supported by the Monash Graduate Scholarship (MGS) and Monash International Tuition Scholarship (MITS). FSM was supported under an ARC Discovery Early Career Research Award (DECRA; DE210101433); RSJ was supported under a DECRA (DE210101923). This research has been supported by Horizon 2020 (PROTECT Grant 869304). Open access publishing facilitated by Monash University, as part of the Wiley - Monash University agreement via the Council of Australian University Librarians.

### References

- Alley, K., Scambos, T., Miller, J., Long, D., & MacFerrin, M. (2018). Quantifying vulnerability of Antarctic ice shelves to hydrofracture using microwave scattering properties. *Remote Sensing of Environment*, 210, 297–306. <https://doi.org/10.1016/j.rse.2018.03.025>
- Arblaster, J. M., & Meehl, G. A. (2006). Contributions of external forcings to Southern Annular Mode trends. *Journal of Climate*, 19(12), 2896–2905. <https://doi.org/10.1175/JCLI3774.1>
- Arblaster, J. M., Meehl, G. A., & Karoly, D. J. (2011). Future climate change in the Southern Hemisphere: Competing effects of ozone and greenhouse gases. *Geophysical Research Letters*, 38(2), L02701. <https://doi.org/10.1029/2010GL045384>
- Arthur, J. F., Stokes, C., Jamieson, S. S., Carr, J. R., & Leeson, A. A. (2020). Recent understanding of Antarctic supraglacial lakes using satellite remote sensing. *Progress in Physical Geography: Earth and Environment*, 44(6), 837–869. <https://doi.org/10.1177/0309133320916114>
- Arthur, J. F., Stokes, C. R., Jamieson, S. S. R., Miles, B. W. J., Carr, J. R., & Leeson, A. A. (2021). The triggers of the disaggregation of Voyeykov Ice Shelf (2007), Wilkes Land, East Antarctica, and its subsequent evolution. *Journal of Glaciology*, 67(265), 933–951. <https://doi.org/10.1017/jog.2021.45>
- Banwell, A. F., MacAyeal, D. R., & Sergienko, O. V. (2013). Breakup of the Larsen B Ice Shelf triggered by chain reaction drainage of supraglacial lakes. *Geophysical Research Letters*, 40(22), 5872–5876. <https://doi.org/10.1002/2013GL057694>
- Banwell, A. F., Wever, N., Dunmire, D., & Picard, G. (2023). Quantifying Antarctic-wide ice-shelf surface melt volume using microwave and firn model data: 1980 to 2021. *Geophysical Research Letters*, 50(12), e2023GL102744. <https://doi.org/10.1029/2023GL102744>
- Bindschadler, R., Choi, H., Wichlacz, A., Bingham, R., Bohlander, J., Brunt, K., et al. (2011). Getting around Antarctica: New high-resolution mappings of the grounded and freely-floating boundaries of the Antarctic Ice Sheet created for the International Polar Year. *The Cryosphere*, 5(3), 569–588. <https://doi.org/10.5194/tc-5-569-2011>
- Box, J. E., Wehrle, A., van As, D., Fausto, R. S., Kjeldsen, K. K., Dachauer, A., et al. (2022). Greenland Ice Sheet rainfall, heat and albedo feedback impacts from the mid-August 2021 atmospheric river. *Geophysical Research Letters*, 49(11), e2021GL097356. <https://doi.org/10.1029/2021GL097356>
- Braithwaite, R. J., & Olesen, O. B. (1990). Response of the energy balance on the margin of the Greenland Ice Sheet to temperature changes. *Journal of Glaciology*, 36(123), 217–221. <https://doi.org/10.3189/S0022143000009461>
- Campitelli, E., Díaz, L. B., & Vera, C. (2022). Assessment of zonally symmetric and asymmetric components of the Southern Annular Mode using a novel approach. *Climate Dynamics*, 58(1–2), 161–178. <https://doi.org/10.1007/s00382-021-05896-5>
- Cape, M. R., Vernet, M., Skvarca, P., Marinsek, S., Scambos, T., & Domack, E. (2015). Foehn winds link climate-driven warming to ice shelf evolution in Antarctica. *Journal of Geophysical Research: Atmospheres*, 120(21). <https://doi.org/10.1002/2015JD023465>
- Deng, K., Azorin-Molina, C., Yang, S., Hu, C., Zhang, G., Minola, L., & Chen, D. (2022). Changes of Southern Hemisphere westerlies in the future warming climate. *Atmospheric Research*, 270, 106040. <https://doi.org/10.1016/j.atmosres.2022.106040>
- Fogt, R. L., Jones, J. M., & Renwick, J. (2012). Seasonal zonal asymmetries in the Southern Annular Mode and their impact on regional temperature anomalies. *Journal of Climate*, 25(18), 6253–6270. <https://doi.org/10.1175/JCLI-D-11-00474.1>
- Fogt, R. L., & Marshall, G. J. (2020). The Southern Annular Mode: Variability, trends, and climate impacts across the Southern Hemisphere. *WIREs Climate Change*, 11(4), e652. <https://doi.org/10.1002/wcc.652>
- Frerebeau, N., Lebrun, B., Arel-Bundock, V., & Stervbo, U. (2024). Khroma: Colour schemes for scientific data visualization [Software]. Université Bordeaux Montaigne. Pessac, France. <https://doi.org/10.5281/zenodo.1472077>
- Fürst, J. J., Durand, G., Gillet-Chaulet, F., Tavaré, L., Rankl, M., Braun, M., & Gagliardini, O. (2016). The safety band of Antarctic ice shelves. *Nature Climate Change*, 6(5), 479–482. <https://doi.org/10.1038/nclimate2912>
- Gilbert, E., & Kittel, C. (2021). Surface melt and runoff on Antarctic ice shelves at 1.5°C, 2°C, and 4°C of future warming. *Geophysical Research Letters*, 48(8), e2020GL091733. <https://doi.org/10.1029/2020GL091733>
- Goyal, R., Jucker, M., Gupta, A. S., & England, M. H. (2022). A new zonal wave-3 index for the Southern Hemisphere. *Journal of Climate*, 35(15), 5137–5149. <https://doi.org/10.1175/JCLI-D-21-0927.1>
- Hersbach, H., Bell, B., Berrisford, P., Hirahara, S., Horányi, A., Muñoz-Sabater, J., et al. (2020). The ERA5 global reanalysis. *Quarterly Journal of the Royal Meteorological Society*, 146(730), 1999–2049. <https://doi.org/10.1002/qj.3803>
- Hijmans, R. J., Bivand, R., Pebesma, E., & Sumner, M. D. (2023). Terra: Spatial data analysis [Software]. Retrieved from [https://rspatial.org/](https://rspatial.org/hock, R. (2005). Glacier melt: A review of processes and their modelling. Progress in Physical Geography: Earth and Environment, 29(3), 362–391. https://doi.org/10.1191/0309133305pp453ra)
- Hui, F., Ci, T., Cheng, X., Scambo, T. A., Liu, Y., Zhang, Y., et al. (2014). Mapping blue-ice areas in Antarctica using ETM+ and MODIS data. *Annals of Glaciology*, 55(66), 129–137. <https://doi.org/10.3189/2014AoG66A069>
- Jakobs, C. L., Reijmer, C. H., van de Broeke, M. R., van de Berg, W. J., & van Wessem, J. M. (2021). Spatial variability of the snowmelt-albedo feedback in Antarctica. *Journal of Geophysical Research: Earth Surface*, 126(2), e2020JF005696. <https://doi.org/10.1029/2020JF005696>
- Johnson, A., Hock, R., & Fahnestock, M. (2022). Spatial variability and regional trends of Antarctic ice shelf surface melt duration over 1979–2020 derived from passive microwave data. *Journal of Glaciology*, 68(269), 533–546. <https://doi.org/10.1017/jog.2021.112>

- King, J., Anchukaitis, K. J., Allen, K., Vance, T., & Hessler, A. (2023). Trends and variability in the Southern Annular Mode over the common era. *Nature Communications*, 14(1), 2324. <https://doi.org/10.1038/s41467-023-37643-1>
- Kittel, C., Amory, C., Agosta, C., Jourdain, N. C., Hofer, S., Delhasse, A., et al. (2021). Diverging future surface mass balance between the Antarctic ice shelves and grounded ice sheet. *The Cryosphere*, 15(3), 1215–1236. <https://doi.org/10.5194/tc-15-1215-2021>
- Laffin, M. K., Zender, C. S., van Wessem, M., & Marinsek, S. (2022). The role of föhn winds in eastern Antarctic Peninsula rapid ice shelf collapse. *The Cryosphere*, 16(4), 1369–1381. <https://doi.org/10.5194/tc-16-1369-2022>
- Lai, C.-Y., Kingslake, J., Wearing, M. G., Chen, P.-H. C., Gentine, P., Li, H., et al. (2020). Vulnerability of Antarctica's ice shelves to meltwater-driven fracture. *Nature*, 584(7822), 574–578. <https://doi.org/10.1038/s41586-020-2627-8>
- Leeson, A. A., Forster, E., Rice, A., Gourmelen, N., & van Wessem, J. M. (2020). Evolution of supraglacial lakes on the Larsen B Ice Shelf in the decades before it collapsed. *Geophysical Research Letters*, 47(4), e2019GL085591. <https://doi.org/10.1029/2019GL085591>
- Lenaerts, J. T. M., Lhermitte, S., Drews, R., Ligtenberg, S. R. M., Berger, S., Helm, V., et al. (2017). Meltwater produced by wind–albedo interaction stored in an East Antarctic ice shelf. *Nature Climate Change*, 7(1), 58–62. <https://doi.org/10.1038/nclimate3180>
- Lenaerts, J. T. M., Ligtenberg, S. R. M., Medley, B., van den Berg, W. J., Konrad, H., Nicolas, J. P., et al. (2018). Climate and surface mass balance of coastal West Antarctica resolved by regional climate modelling. *Annals of Glaciology*, 59(76pt1), 29–41. <https://doi.org/10.1017/aog.2017.42>
- Lenaerts, J. T. M., van den Broeke, M. R., Scarchilli, C., & Agosta, C. (2012). Impact of model resolution on simulated wind, drifting snow and surface mass balance in Terre Adélie, East Antarctica. *Journal of Glaciology*, 58(211), 821–829. <https://doi.org/10.3189/2012JG12J020>
- Lhermitte, S., Wouters, B., & HiRISE Team. (2023). The triggers for Conger Ice Shelf demise: Long-term weakening vs. short-term collapse. In *EGU General Assembly 2023. Vienna, Austria*. <https://doi.org/10.5194/egusphere-egu23-16400>
- Ligtenberg, S. R. M., Kuipers Munneke, P., & van den Broeke, M. R. (2014). Present and future variations in Antarctic firm air content. *The Cryosphere*, 8(5), 1711–1723. <https://doi.org/10.5194/tc-8-1711-2014>
- MacAyeal, D. R., Scambos, T. A., Hulbe, C. L., & Fahnestock, M. A. (2003). Catastrophic ice-shelf break-up by an ice-shelf-fragment-capsize mechanism. *Journal of Glaciology*, 49(164), 22–36. <https://doi.org/10.3189/172756503781830863>
- Marshall, G. J. (2003). Trends in the Southern Annular Mode from observations and reanalyses. *Journal of Climate*, 16(24), 4134–4143. [https://doi.org/10.1175/1520-0442\(2003\)016\(4134:TTSAM\)2.0.CO;2](https://doi.org/10.1175/1520-0442(2003)016(4134:TTSAM)2.0.CO;2)
- Marshall, G. J., Orr, A., van Lipzig, N. P. M., & King, J. C. (2006). The impact of a changing Southern Hemisphere Annular Mode on Antarctic Peninsula summer temperatures. *Journal of Climate*, 19(20), 5388–5404. <https://doi.org/10.1175/JCLI3844.1>
- Marshall, G. J., & Thompson, D. W. J. (2016). The signatures of large-scale patterns of atmospheric variability in Antarctic surface temperatures. *Journal of Geophysical Research: Atmospheres*, 121(7), 3276–3289. <https://doi.org/10.1002/2015JD024665>
- Mo, K. C. (2000). Relationships between low-frequency variability in the Southern Hemisphere and sea surface temperature anomalies. *Journal of Climate*, 13(20), 3599–3610. [https://doi.org/10.1175/1520-0442\(2000\)013\(3599:RBLFV1\)2.0.CO;2](https://doi.org/10.1175/1520-0442(2000)013(3599:RBLFV1)2.0.CO;2)
- Morlighem, M., Rignot, E., Binder, T., Blankenship, D., Drews, R., Eagles, G., et al. (2020). Deep glacial troughs and stabilizing ridges unveiled beneath the margins of the Antarctic Ice Sheet. *Nature Geoscience*, 13(2), 132–137. <https://doi.org/10.1038/s41561-019-0510-8>
- Morris, E. M., & Vaughan, D. G. (2003). *Spatial and temporal variation of surface temperature on the Antarctic Peninsula and the limit of viability of ice shelves*. In E. Domack, A. Levente, A. Burnet, R. Bindshadler, P. Convey, & M. Kirby (Eds.), *Antarctic Research Series* (pp. 61–68). American Geophysical Union. <https://doi.org/10.1029/AR079p0061>
- Mouginot, J., Scheuchl, B., & Rignot, E. (2017). MEaSURES Antarctic Boundaries for IPY 2007–2009 from Satellite Radar, Version 2. [Dataset]. NASA National Snow and Ice Data Center Distributed Active Archive Center. <https://doi.org/10.5067/AXE4121732AD>
- Munneke, P. K., Ligtenberg, S. R. M., van den Broeke, M. R., & Vaughan, D. G. (2014). Firm air depletion as a precursor of Antarctic ice-shelf collapse. *Journal of Glaciology*, 60(220), 205–214. <https://doi.org/10.3189/2014JG131183>
- Neme, J., England, M. H., & McC. Hogg, A. (2022). Projected changes of surface winds over the Antarctic continental margin. *Geophysical Research Letters*, 49(16), e2022GL098820. <https://doi.org/10.1029/2022GL098820>
- Nghiem, S. V., Hall, D. K., Mote, T. L., Tedesco, M., Albert, M. R., Keegan, K., et al. (2012). The extreme melt across the Greenland Ice Sheet in 2012. *Geophysical Research Letters*, 39(20), L20502. <https://doi.org/10.1029/2012GL053611>
- Nicola, L., Notz, D., & Winkelmann, R. (2023). Revisiting temperature sensitivity: How does Antarctic precipitation change with temperature? *The Cryosphere*, 17(7), 2563–2583. <https://doi.org/10.5194/tc-17-2563-2023>
- Nicolas, J. P., Vogelmann, A. M., Scott, R. C., Wilson, A. B., Cadetdu, M. P., Bromwich, D. H., et al. (2017). 2016 Extensive summer melt in West Antarctica favoured by strong El Niño. *Nature Communications*, 8(1), 15799. <https://doi.org/10.1038/ncomms15799>
- Ohmura, A. (2001). Physical basis for the temperature-based melt-index method. *Journal of Applied Meteorology and Climatology*, 40(4), 753–761. [https://doi.org/10.1175/1520-0450\(2001\)040\(0753:PBFTTB\)2.0.CO;2](https://doi.org/10.1175/1520-0450(2001)040(0753:PBFTTB)2.0.CO;2)
- Oppenheimer, M., Glavovic, B., Hinkel, J., van de Wal, R., Magnan, A., Abd-Elgawad, A., et al. (2019). *Sea level rise and implication for low-lying Islands, coasts and communities*. In H.-O. Portner, & et al. (Eds.), *IPCC special report on the ocean and cryosphere in a changing climate* (pp. 321–445). Cambridge University Press. <https://doi.org/10.1017/9781009157964.006>
- Orr, A., Deb, P., Clem, K. R., Gilbert, E., Bromwich, D. H., Boberg, F., et al. (2023). Characteristics of surface “Melt Potential” over Antarctic ice shelves based on regional atmospheric model simulations of summer air temperature extremes from 1979/80 to 2018/19. *Journal of Climate*, 36(10), 3357–3383. <https://doi.org/10.1175/JCLI-D-22-0386.1>
- Pfeffer, W. T., Meier, M. F., & Illangasekare, T. H. (1991). Retention of Greenland runoff by refreezing: Implications for projected future sea level change. *Journal of Geophysical Research: Oceans*, 96(C12), 22117–22124. <https://doi.org/10.1029/91JC02502>
- Picard, G. (2022). Snow status (Wet/Dry) in Antarctica from SMMR, SSM/I, AMSR-E and AMSR2 passive microwave radiometers. [dataset]. PerSCiDO. <https://doi.org/10.18709/PERSCIDO.2022.09.DS376>
- Picard, G., Domine, F., Krinner, G., Arnaud, L., & Lefebvre, E. (2012). Inhibition of the positive snow-albedo feedback by precipitation in interior Antarctica. *Nature Climate Change*, 2(11), 795–798. <https://doi.org/10.1038/nclimate1590>
- Polvani, L. M., Waugh, D. W., Correa, G. J. P., & Son, S.-W. (2011). Stratospheric ozone depletion: The main driver of twentieth-century atmospheric circulation changes in the Southern Hemisphere. *Journal of Climate*, 24(3), 795–812. <https://doi.org/10.1175/2010JCLI3772.1>
- Previdi, M., Smith, K. L., & Polvani, L. M. (2013). The Antarctic atmospheric energy budget. Part I: Climatology and intraseasonal-to-interannual variability. *Journal of Climate*, 26(17), 6406–6418. <https://doi.org/10.1175/JCLI-D-12-00640.1>
- Raphael, M. N. (2004). A zonal wave 3 index for the Southern Hemisphere. *Geophysical Research Letters*, 31(23), L23212. <https://doi.org/10.1029/2004GL020365>
- R Core Team. (2023). R: A language and environment for statistical computing [Software]. Retrieved from <https://www.R-project.org/>
- Reese, R., Gudmundsson, G. H., Levermann, A., & Winkelmann, R. (2018). The far reach of ice-shelf thinning in Antarctica. *Nature Climate Change*, 8(1), 53–57. <https://doi.org/10.1038/s41558-017-0020-x>

- Rignot, E., Jacobs, S., Mouginot, J., & Scheuchl, B. (2013). Ice-shelf melting around Antarctica. *Science*, *341*(6143), 266–270. <https://doi.org/10.1126/science.1235798>
- Robel, A. A., & Banwell, A. F. (2019). A speed limit on ice shelf collapse through hydrofracture. *Geophysical Research Letters*, *46*(21), 12092–12100. <https://doi.org/10.1029/2019GL084397>
- Robinson, W. A. (2000). A baroclinic mechanism for the eddy feedback on the zonal index. *Journal of the Atmospheric Sciences*, *57*(3), 415–422. [https://doi.org/10.1175/1520-0469\(2000\)057<0415:ABMFTE>2.0.CO;2](https://doi.org/10.1175/1520-0469(2000)057<0415:ABMFTE>2.0.CO;2)
- Saunderson, D., Mackintosh, A., McCormack, F., Jones, R. S., & Picard, G. (2022). Surface melt on the Shackleton Ice Shelf, East Antarctica (2003–2021). *The Cryosphere*, *16*(10), 4553–4569. <https://doi.org/10.5194/tc-16-4553-2022>
- Scambos, T., Fricker, H. A., Liu, C.-C., Bohlander, J., Fastook, J., Sargent, A., et al. (2009). Ice shelf disintegration by plate bending and hydrofracture: Satellite observations and model results of the 2008 Wilkins Ice Shelf break-ups. *Earth and Planetary Science Letters*, *280*(1–4), 51–60. <https://doi.org/10.1016/j.epsl.2008.12.027>
- Scambos, T., Hulbe, C., Fahnestock, M., & Bohlander, J. (2000). The link between climate warming and break-up of ice shelves in the Antarctic Peninsula. *Journal of Glaciology*, *46*(154), 516–530. <https://doi.org/10.3189/172756500781833043>
- Scott, R. C., Nicolas, J. P., Bromwich, D. H., Norris, J. R., & Lubin, D. (2019). Meteorological drivers and large-scale climate forcing of West Antarctic surface melt. *Journal of Climate*, *32*(3), 665–684. <https://doi.org/10.1175/JCLI-D-18-0233.1>
- Simpkins, G. R., & Karpechko, A. Y. (2012). Sensitivity of the Southern Annular Mode to greenhouse gas emission scenarios. *Climate Dynamics*, *38*(3–4), 563–572. <https://doi.org/10.1007/s00382-011-1121-2>
- Sun, S., Pattyn, F., Simon, E. G., Albrecht, T., Cornford, S., Calov, R., et al. (2020). Antarctic Ice Sheet response to sudden and sustained ice-shelf collapse (ABUMIP). *Journal of Glaciology*, *66*(260), 891–904. <https://doi.org/10.1017/jog.2020.67>
- Tedesco, M., Abdalati, W., & Zwally, H. J. (2007). Persistent surface snowmelt over Antarctica (1987–2006) from 19.35 GHz brightness temperatures. *Geophysical Research Letters*, *34*(18), L18504. <https://doi.org/10.1029/2007GL031199>
- Tedesco, M., & Monaghan, A. J. (2009). An updated Antarctic melt record through 2009 and its linkages to high-latitude and tropical climate variability. *Geophysical Research Letters*, *36*(18), L18502. <https://doi.org/10.1029/2009GL039186>
- Torinesi, O., Fily, M., & Genthon, C. (2003). Variability and trends of the summer melt period of Antarctic ice margins since 1980 from microwave sensors. *Journal of Climate*, *16*(7), 1047–1060. [https://doi.org/10.1175/1520-0442\(2003\)016<1047:VATOTS>2.0.CO;2](https://doi.org/10.1175/1520-0442(2003)016<1047:VATOTS>2.0.CO;2)
- Trusel, L. D., Frey, K. E., Das, S. B., Karnauskas, K. B., Kuipers Munneke, P., van Meijgaard, E., & van den Broeke, M. R. (2015). Divergent trajectories of Antarctic surface melt under two twenty-first-century climate scenarios. *Nature Geoscience*, *8*(12), 927–932. <https://doi.org/10.1038/ngeo2563>
- Trusel, L. D., Frey, K. E., Das, S. B., Munneke, P. K., & van den Broeke, M. R. (2013). Satellite-based estimates of Antarctic surface meltwater fluxes. *Geophysical Research Letters*, *40*(23), 6148–6153. <https://doi.org/10.1002/2013GL058138>
- van den Broeke, M. R., & van Lipzig, N. P. M. (2004). Changes in Antarctic temperature, wind and precipitation in response to the Antarctic Oscillation. *Annals of Glaciology*, *39*, 119–126. <https://doi.org/10.3189/172756404781814654>
- van der Veen, C. J. (1998). Fracture mechanics approach to penetration of surface crevasses on glaciers. *Cold Regions Science and Technology*, *27*(1), 31–47. [https://doi.org/10.1016/S0165-232X\(97\)00022-0](https://doi.org/10.1016/S0165-232X(97)00022-0)
- van Dalum, C. T., van de Berg, W. J., Lhermitte, S., & van den Broeke, M. R. (2020). Evaluation of a new snow albedo scheme for the Greenland Ice Sheet in the Regional Atmospheric Climate Model (RACMO2). *The Cryosphere*, *14*(11), 3645–3662. <https://doi.org/10.5194/tc-14-3645-2020>
- van Dalum, C. T., van de Berg, W. J., Libois, Q., Picard, G., & van den Broeke, M. R. (2019). A module to convert spectral to narrowband snow albedo for use in climate models: SNOWBAL v1.2. *Geoscientific Model Development*, *12*(12), 5157–5175. <https://doi.org/10.5194/gmd-12-5157-2019>
- van Dalum, C. T., van de Berg, W. J., & van den Broeke, M. (2021). RACMO2.3p3 monthly SMB, SEB and t2m data for Antarctica (1979–2018). [dataset]. Zenodo. <https://doi.org/10.5281/ZENODO.7639053>
- van Dalum, C. T., van de Berg, W. J., & van den Broeke, M. R. (2022). Sensitivity of Antarctic surface climate to a new spectral snow albedo and radiative transfer scheme in RACMO2.3p3. *The Cryosphere*, *16*(3), 1071–1089. <https://doi.org/10.5194/tc-16-1071-2022>
- van Wessem, J. M., Reijmer, C. H., Lenaerts, J. T. M., van de Berg, W. J., van den Broeke, M. R., & van Meijgaard, E. (2014). Updated cloud physics in a regional atmospheric climate model improves the modelled surface energy balance of Antarctica. *The Cryosphere*, *8*(1), 125–135. <https://doi.org/10.5194/tc-8-125-2014>
- van Wessem, J. M., van de Berg, W. J., Noël, B. P. Y., van Meijgaard, E., Amory, C., Birnbaum, G., et al. (2018). Modelling the climate and surface mass balance of polar ice sheets using RACMO2 – Part 2: Antarctica (1979–2016). *The Cryosphere*, *12*(4), 1479–1498. <https://doi.org/10.5194/tc-12-1479-2018>
- van Wessem, J. M., van den Broeke, M. R., Wouters, B., & Lhermitte, S. (2023). Variable temperature thresholds of melt pond formation on Antarctic ice shelves. *Nature Climate Change*, *13*(2), 161–166. <https://doi.org/10.1038/s41558-022-01577-1>
- Weertman, J. (1973). *Can a water-filled crevasse reach the bottom surface of a glacier?* (pp. 139–145). International Association of Scientific Hydrology Publication.
- Wickham, H., Hester, J., Chang, W., Bryan, J., & RStudio (2022). Devtools: Tools to make developing R packages easier [Software]. Retrieved from <https://devtools.r-lib.org>
- Wille, J. D., Alexander, S. P., Amory, C., Baiman, R., Barthélemy, L., Bergstrom, D. M., et al. (2024). The extraordinary March 2022 East Antarctica “heat” wave. Part II: Impacts on the Antarctic Ice Sheet. *Journal of Climate*, *37*(3), 779–799. <https://doi.org/10.1175/JCLI-D-23-0176.1>
- Wille, J. D., Favier, V., Dufour, A., Gorodetskaya, I. V., Turner, J., Agosta, C., & Codron, F. (2019). West Antarctic surface melt triggered by atmospheric rivers. *Nature Geoscience*, *12*(11), 911–916. <https://doi.org/10.1038/s41561-019-0460-1>
- Wille, J. D., Favier, V., Jourdain, N. C., Kittel, C., Turton, J. V., Agosta, C., et al. (2022). Intense atmospheric rivers can weaken ice shelf stability at the Antarctic Peninsula. *Communications Earth & Environment*, *3*(1), 90. <https://doi.org/10.1038/s43247-022-00422-9>
- Wiscombe, W. J., & Warren, S. G. (1980). A model for the spectral albedo of snow. I: Pure snow. *Journal of the Atmospheric Sciences*, *37*(12), 2712–2733. [https://doi.org/10.1175/1520-0469\(1980\)037<2712:AMFTSA>2.0.CO;2](https://doi.org/10.1175/1520-0469(1980)037<2712:AMFTSA>2.0.CO;2)
- Zheng, F. (2024). Slowing down of the summer Southern Hemisphere Annular Mode trend against the background of ozone recovery. *Atmospheric and Oceanic Science Letters*, *17*(1), 100375. <https://doi.org/10.1016/j.aosl.2023.100375>
- Zou, X., Bromwich, D. H., Nicolas, J. P., Montenegro, A., & Wang, S.-H. (2019). West Antarctic surface melt event of January 2016 facilitated by föhn warming. *Quarterly Journal of the Royal Meteorological Society*, *145*(719), 687–704. <https://doi.org/10.1002/qj.3460>